Published online 25 November 2021

Nucleic Acids Research, 2022, Vol. 50, No. 3 ***e18***
https://doi.org/10.1093/nar/gkab1117

Isocratic HPLC analysis for the simultaneous determination of dNTPs, rNTPs and ADP in biological samples

Farahnaz Ranjbarian†, Sushma Sharma†, Giulia Falappa, Walter Taruschio, Andrei Chabes and Anders Hofer*

Dept. Medical Biochemistry and Biophysics, Umeå University, SE-901 87 Umeå, Sweden

Received July 01, 2021; Revised September 22, 2021; Editorial Decision October 20, 2021; Accepted October 26, 2021

ABSTRACT

Information about the cellular concentrations of deoxyribonucleoside triphosphates (dNTPs) is instrumental for mechanistic studies of DNA replication and for understanding diseases caused by defects in dNTP metabolism. The dNTPs are measured by methods based on either HPLC or DNA polymerization. An advantage with the HPLC-based techniques is that the parallel analysis of ribonucleoside triphosphates (rNTPs) can serve as an internal quality control of nucleotide integrity and extraction efficiency. We have developed a Freon-free trichloroacetic acid-based method to extract cellular nucleotides and an isocratic reverse phase HPLC-based technique that is able to separate dNTPs, rNTPs and ADP in a single run. The ability to measure the ADP levels improves the control of nucleotide integrity, and the use of an isocratic elution overcomes the shifting baseline problems in previously developed gradient-based reversed phase protocols for simultaneously measuring dNTPs and rNTPs. An optional DNA-polymerase-dependent step is used for confirmation that the dNTP peaks do not overlap with other components of the extracts, further increasing the reliability of the analysis. The method is compatible with a wide range of biological samples and has a sensitivity better than other UV-based HPLC protocols, closely matching that of mass spectrometry-based detection.

GRAPHICAL ABSTRACT

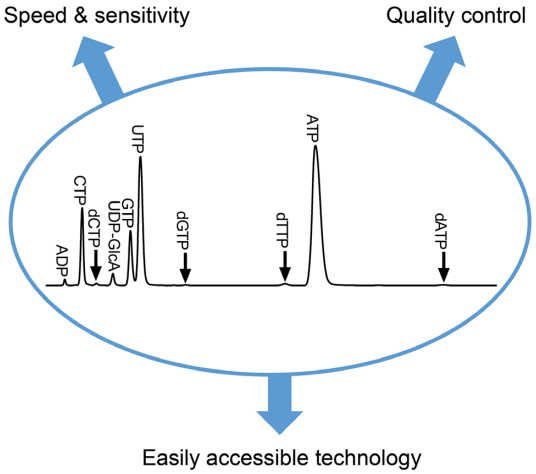

INTRODUCTION

Balanced pools of deoxribonucleoside triphosphates (dNTPs) are important for DNA replication fidelity (1–4). The levels of dNTPs vary between different species, cell types, and growth phases, but in mammalian cells they are typically 2–3 orders of magnitude lower than the corresponding ribonucleotides (rNTPs) (5,6), and this makes their analysis challenging. The DNA polymerase-based techniques are becoming more popular due to their ability to measure many samples simultaneously, and thereby improve the throughput (7–9). However, these assays are indirect and can be affected by other components of the extracts such as rNTPs (10,11). Analyses of extracts from cells treated with deoxynucleoside analogues that are commonly used as anticancer and antiviral agents can be particularly difficult because the phosphorylated analogues can interfere with the assay. HPLC-based methods have the advantages of both being direct and able to measure rNTPs (12), which in contrast to dNTPs do not fluctuate

*To whom correspondence should be addressed. Tel: +46 70 2974096; Email: anders.hofer@umu.se
†The authors wish it to be known that, in their opinion, the first two authors should be regarded as Joint First Authors.

during the cell cycle and therefore can serve as controls for the extraction efficiency and sample handling. It is an advantage if the HPLC method also can measure ADP because the ATP:ADP ratio shows whether the energy charge was affected by the harvesting procedure.

The HPLC-based methods available for dNTP and rNTP analysis differ by cell extraction technique, column type, and detector (12). Most of them start with cell extraction using acids or organic solvents. The generated crude extracts are generally dominated by rNTPs, which in anion exchange HPLC protocols need to be captured by boronate resins or selectively degraded with periodate treatment in order to allow the detection of the much less abundant dNTPs (13,14). A separate HPLC analysis of crude extracts is in this case necessary for the measurement of the rNTP pool. Using reverse phase chromatography and a tetrabutylammonium (TBA) salt as an ion pairing agent in the mobile phase, it has been possible to analyze dNTPs, rNTPs and ADP in a single run (15–17). These methods work well for the determination of ADP, rNTPs, and various nucleotide-conjugated sugars that are abundant in cell extracts, but they suffer from unstable baselines due to non-isocratic elution and lack of proper controls to discriminate dNTPs from other small peaks in the cell extracts. Mass spectrometry-based detection makes it possible to overcome these problems and to achieve much higher sensitivity than with UV detection (5). However, a limitation of mass spectrometry-based techniques is the requirement for expensive equipment to perform the analyses. In the current work, we have created a high-sensitivity method based on isocratic reverse phase chromatography, UV detection, and a DNA-polymerase-based approach to discriminate dNTPs from background peaks. The new method can measure dNTPs, rNTPs, and ADP from a wide range of extracts with a sensitivity close to mass spectrometry-based detection.

MATERIALS AND METHODS

Reagents

Chemicals for the HPLC mobile phase included HPLC-grade methanol (MeOH) and acetonitrile (ACN) from Thermo Fischer Scientific, Waltham, MA, USA (#M/4056/17X and #A0626/17X, respectively), tetrabutylammonium bromide (TBA-Br) for ion pair chromatography from Merck, Darmstadt, Germany (#86857), and HiPerSolv Chromanorm-grade KH_2PO_4 from VWR International, Radnor, PA, USA (#153184U). For extraction and preparation of cellular nucleotides, we used HPLC-grade ACN and MeOH (see above), trichloroacetic acid (TCA) from Scharlab S. L., Sentmenat, Spain (#AC31321000), OASIS solid phase extraction (SPE) columns with weak anion exchange (WAX) resin from Waters Corporation, Milford, MA, USA (#186002492) and Lichropur ammonia solution (25%) for HPLC from Merck (#5.43830.0250). For the DNA polymerase assay, we used M13 mp18 ss-DNA (250 μg/ml) from New England Biolabs, Ipswich, MA, USA (#N4040S), random decamers from Thermo Fischer Scientific (#AM5722G), and Klenow Fragment Exo$^-$ (5 U/μl) from Thermo Fischer Scientific (#EP0421).

Biological resources

The cell lines used were *Saccharomyces cerevisiae* strain AC402 (MATalpha ade2-1 his3-11,15 leu2-3,112 trp1-1 ura3-1 RAD5 + CAN1), mouse Balb/3T3 fibroblasts (ATCC no CCL-163) and *Trypanosoma brucei* Lister 427 (http://tryps.rockefeller.edu/trypsru2_pedigrees.html). Animal experiments on C57BL/6 mouse embryos were approved by the Animal Review Board at the Court of Appeal of Northern Norrland (Umeå, Sweden).

HPLC equipment, detector settings, loop sizes and columns

The HPLC experiments were performed by using three Smartline Pump 1000s (Knauer, Berlin, Germany) with the inlets connected to an ERC 3145α solvent degasser (Knauer). The outlets of the pumps were connected to a Dynamic Mixing Chamber (Knauer) and a Cheminert C82VH-1676 injector connected to the column. The column was protected by a Sunshell guard cartridge (ChromaNik Technologies Inc., Osaka, Japan). The outlet of the column was connected to a UV2075 Plus detector (Jasco International Co. Ltd, Hachioji, Japan). Unless otherwise specified, the UV detector was set to a wavelength of 270 nm using the standard setting (STD = 5 s update time), CR filter, and an output of 1 V/0.1 AU. The fast response setting (FAST = 3 s), which gives higher noise, was only used when analyzing the effect of the flow rate on resolution and for gradient elution. An injection loop of 100 μl was generally used for 4.6 mm ID columns, unless otherwise specified. The temperature of the column was controlled with a 300 mm HotPocket heater (Thermo Fischer Scientific). Most experiments were performed with a 4.6 mm × 150 mm Sunshell C18-WP 2.6 μm column (ChromaNik Technologies Inc.). However, initially we also used different ACE Excel 2 μm variants – C18, C18-AR and C18-PFP (Advanced Chromatography Technologies Inc., Aberdeen, Scotland, UK) – with dimensions specified in the figure legends.

HPLC mobile phase

Three solutions were prepared for the mobile phase, solution A, B and C. In our final protocols, one liter of solution A contained 23 g KH_2PO_4 (HiPerSolv Chromanorm, VWR), 45.6 g ACN (5.8% v/v) and 1.27 ml 4 M KOH to reach a pH of 5.6. Solution B was 5.8% ACN, and solution C was 3.5 g/l TBA-Br in 5.8% ACN. It was important to use chromatography-grade KH_2PO_4 and TBA-Br for the stability of the columns. In addition, we prepared 5× buffer A and 20× buffer C solutions but without ACN as ingredients for making a 10× loading solution. The 5× buffer A solution contained 11.5 g KH_2PO_4 and 0.6375 ml 4M KOH per 100 ml, and the 20× solution C contained 1.4 g TBA-Br/100 ml. For the standard HPLC protocols, we mixed equal amounts of these two solutions to make a 10× loading solution.

Final HPLC protocols

Two final HPLC protocols were developed using a 4.6 × 150 mm Sunshell C18-WP 2.6 μm column and a flow rate of 1.2 ml/min (Table 1). The High-Resolution Protocol is the

Table 1. Summary of HPLC protocols and cell extraction methods. Abbreviations used are ACN: acetonitrile, KP_i: potassium phosphate (KH_2PO_4, pH-adjusted with KOH), TBA-Br: tetrabutylammonium bromide, TCA: trichloroacetic acid, TFA: trifluoroacetic acid, C-TOA: chloroform-trioctylamine mixture, WAX-SPE: weak anion exchange - solid phase extraction.

Protocols	Conditions	Features
HPLC		
High-resolution protocol	5.8% ACN, 0.7 g/l TBA-Br, ∼8.7 g/l KP_i[a] pH 5.6, T = ambient	1. Measures ADP, rNTPs, dNTPs and dUTP 2. Compatible with all extraction solutions
Fast protocol	5.8% ACN, 0.7 g/l TBA-Br, ∼9.7 g/l KP_i[a] pH 5.6, $T = 30°C$	1. Shorter analysis tim 2. Measures ADP, rNTPs, dNTPs (but not dUTP) 3. Less compatible with TCA (due to t-peak)
Cell extraction		
Acid extraction (TCA/TFA)	10–12% TCA/TFA + 15 mM $MgCl_2$ Cleanup: C-TOA + WAX-SPE	1. Strong extraction, but gives extra peaks 2. TFA improves chromatograms (no t-peak) 3. C-TOA is Freon-free
Organic solvents (ACN/MeOH)	50% ACN or 80% MeOH Cleanup: only WAX-SPE	1. Cleaner chromatograms than with TCA/TFA

[a]The exact KP_i concentration is determined by the optimization of the protocol.

more versatile of the two and can separate all dNTPs, including dUTP, as well as rNTPs and ADP. This method is run at ambient temperature with a mobile phase containing 38–39% A and 20% C (the remaining 42–43% is B). Just before HPLC analysis, samples are mixed with 10 × loading solution (see above) mimicking the mobile phase pH and TBA, but with a lower final concentration of KP_i and no ACN. The Fast Protocol is run at 30°C with a mobile phase containing a mixture of 42–43% A and 20% C (the remaining 37–38% is B). The main advantage with this protocol is that the analysis time is shortened by ∼20%, but it is not able to separate dUTP from dGTP.

The optimal percentage of solution A in the mobile phase is determined by a standard sample containing 1 μM ADP + rNTPs, 0.5 μM dNTPs and 0.25 μM dADP + UDP-glucuronic acid (UDP-GlcA) mixed with 10× loading solution. The dADP peak location should be in the middle between the dCTP and UDP-GlcA peaks. If not, its relative position can be shifted to the left or right by decreasing or increasing the percentage of A in 1% increments, respectively. Correcting the positioning of dADP means that the unknown peaks present in some of the extracts, denoted c and g, will also be well separated from the closest dNTPs. In samples where dADP is very high, which can happen in extracts from cells treated with deoxyadenosine, the percentage of A can be increased in order to position the dADP peak farther away from dCTP, but it is advisable to not increase it by >1% to avoid excessive movements of the unknown peaks.

The high-resolution protocol is versatile and works with all tested types of samples, whereas the fast protocol is not ideally suited for cells extracted with TCA, which contains an impurity denoted t having a retention time close to dTTP. The position of the t-peak needs in this case to be verified by a t-standard prepared as described below. In contrast, the t-peak is positioned far away from dTTP and poses no problem using the High-Resolution Protocol. As the column gets older, the retention times of rNTPs and dNTPs are gradually shortened and the separation of the t-peak from dTTP with the Fast Protocol improves.

The column storage solution is 7% ACN if the column is planned to be used within the next few days and 70% MeOH for long-term storage. After storage with 70% MeOH, the column is run for a few minutes with 7% ACN before using buffer-containing solutions. The equilibration of brand-new columns takes at least 10 h at 0.2 ml/min with the final mobile phase solution in order to achieve full separation of all nucleotides including dUTP and dGTP, whereas 1 h at full speed is generally enough after short-term storage. Whenever chromatography performance decreases, the column is flushed with 70% MeOH for an hour, or if necessary the precolumn is changed. The precolumn is then equilibrated separately for 2 h with mobile phase and washed briefly with 7% ACN for a few minutes before attachment to the main column.

TCA extraction optimization and preparation of the t-standard

Aqueous solutions of TCA are commonly used for cell extraction, and TCA can be removed from the samples in a subsequent step using a mixture of Freon (1,1,2-trifluoro-2,2,1-trichloroethane) and *N*,*N*,*N*-trioctylamine. However, Freon is an ozone-depleting substance and its use in laboratories is highly restricted. Therefore, we tested if Freon could be replaced with chloroform, which has similar chemical properties. For this purpose, nucleotide solutions containing 0.75 μM ADP, 0.5 μM of each dNTP and AMP-PNP, 5 μM CTP, GTP, and UTP, and 20 μM ATP were prepared in 500 μl 10% (w/v) TCA (∼0.6 M) containing 15 mM $MgCl_2$. The samples were subsequently extracted with 720 μl of a 1:0.28 chloroform-trioctylamine solution prepared by mixing 1 ml chloroform with 0.28 ml trioctylamine. Control experiments were performed with 1:0.28 Freon-trioctylamine. After the addition of chloroform-trioctylamine or Freon-trioctylamine to the nucleotide solutions, the tubes were individually vortexed for 30 s and centrifuged for 1 min. The upper phase was transferred to a second tube, and the pH was confirmed to be >5 by spotting 0.2 μl on pH-paper. The vortexing step was critical

for efficient removal of TCA, and it worked better if each tube was vortexed individually. If this step was properly performed and the pH was above 5, it was no longer necessary to perform a second extraction with 500 μl chloroform–trioctylamine or Freon-trioctylamine solution as described in previous protocols (18,19). When transferring the aqueous phase in the extraction procedure, we found it convenient to transfer a fixed volume (in our case 425 μl) instead of the whole volume. In order to know how large a fraction of the whole volume is taken out and then to compensate for that in the final calculation of nucleotides, it is important to consider how much the whole volume shrinks when the acid is removed. Empirically, we determined this factor to be 0.943, which means that the whole volume becomes 471.5 μl (500 × 0.943) after the first extraction. We did not observe such a volume change in the second extraction, which was expected because most of the acid had been removed. Similar experiments were also performed with 0.6 M trifluoroacetic acid (TFA) instead of TCA, and in this case the corresponding shrinkage factor in the first extraction was 0.983.

The samples were further purified by OASIS WAX-SPE essentially as described previously (5). The SPE columns were first equilibrated in a three-step procedure with 2 ml MeOH followed by 2 ml water and 2 ml 50 mM ammonium acetate prepared from acetic acid adjusted to pH 4.6 with ammonia. Each sample was diluted with 2 ml 50 mM ammonium acetate pH 4.6. After application of the diluted sample to the SPE column, the column was washed first with 2 ml 50 mM ammonium acetate pH 4.6 and then with 2 ml of a solution containing 99.5 parts MeOH and 0.5 parts 25% aqueous ammonia solution. The nucleotides were finally eluted with 1.5 ml of a solution consisting of 80 parts MeOH, 15 parts water and 5 parts 25% aqueous ammonia solution. The eluted sample was collected, evaporated in a Speedvac to dryness (∼2 h), resuspended in 200 μl water and stored at –20°C. We found it suitable to use plastic tubes for the Speedvac (75 mm × 12 mm PS tubes, #55.476 from Sarstedt) to minimize sample adherence to the tube walls after resuspension. The samples were analyzed by the HPLC Fast Protocol to monitor nucleotide recoveries. We also prepared the t-standard described above where 500 μl 10% TCA (without $MgCl_2$) was extracted with chloroform-trioctylamine, but in this case without SPE purification because the t-impurity is partially removed by this step.

Mouse embryos

Homozygous *SAMHD1*$^{-/-}$ knockout mice in the C57BL/6 background (20) were mated with WT C57BL/6 mice. Day 11 embryos were isolated from these crosses, and their tails were removed for genotyping (21) before nucleotide extraction as described below.

Cell culture

S. cerevisiae were cultured at 30°C with shaking in Yeast extract Peptone Dextrose (YPD) growth medium supplemented with 0.02 g/l adenine. Mouse Balb/3T3 fibroblasts were grown as monolayers on 10 cm tissue culture dishes with a standard TC surface (#83.3902 from Sarstedt AG & Co., Nümbrecht, Germany). Note that culture dishes with protein coating should be avoided when planning to use TCA as the extracting solution because peptides can be generated from protein degradation under acidic conditions. In contrast, organic extraction solutions can be used with any coating. The cells were cultured in Dulbecco´s Modified Eagle´s Medium (DMEM) supplemented with 10% (v/v) fetal bovine serum, 0.584 g/l L-glutamine, and 100 ml/l 100× penicillin–streptomycin (Thermo Fischer Scientific). *T. brucei* Lister 427 was grown in Hirumi´s modified Iscove´s Medium-9 (HMI-9) (22) but with 10% (v/v) fetal bovine serum instead of the Serum Plus as used in the original protocol (22). The mammalian and *T. brucei* cells were both cultured at 37°C in a humidified atmosphere with 5% CO_2.

Sample extraction

Table 1 summarizes the different types of extraction solutions used in this study. Different extraction techniques were used for *S. cerevisiae*, *T. brucei* and mammalian fibroblasts (Balb/3T3). The *S. cerevisiae* TCA-dependent extraction protocol was a modification of the previously described protocol (19). *S. cerevisiae* cells at OD = 20 (OD = A_{600} × volume in ml), corresponding to 3.7 × 10^8 cells, were harvested in the logarithmic growth phase (4–8 × 10^6 cells/ml) and collected on a 0.8 μm MF Millipore membrane filter (#AAWP02500 from Merck). The filter was washed twice with phosphate-buffered saline (PBS) supplemented with 2% (w/v) glucose and transferred to a 2-ml Eppendorf tube containing 700 μl ice-cold 12% (w/v) TCA supplemented with 15 mM $MgCl_2$. The cells were briefly vortexed, frozen in liquid nitrogen, thawed on ice, vortexed for 30 s in a cold room (∼4°C), and agitated for 20 min as described previously (19). The Eppendorf tube was punctured close to the bottom, inserted into a 2-ml Eppendorf tube, and centrifuged briefly to transfer the solution to the bottom tube. The TCA samples were subsequently extracted with 1.21 ml chloroform-trioctylamine and purified by WAX-SPE as described above. The samples could be stored at –20°C for at least a week both after the completion of the TCA extraction step and after completion of the entire procedure, but because small additional peaks appear over time it is advisable to use –80°C for long-term storage. *T. brucei* and mammalian cell extraction protocols differed from the *S. cerevisiae* only in the harvesting step where scraping or centrifugation, respectively, was used instead of filtering. Logarithmically growing *T. brucei* (50 ml of 2 × 10^6 cells/ml) were chilled on ice, and the liquid was transferred to a 50 ml Falcon tube and centrifuged at 3000 × *g* at 4°C for 5 min. The medium was decanted, and the pellet was resuspended in the remaining liquid in the tube (usually a few hundred μl after decanting) by tapping the bottom of the tube. The cells were transferred to an Eppendorf tube and centrifuged for 1 min at 16 000 × *g* at 4°C. The supernatant was discarded, 500 μl 10% (w/v) TCA with 15 mM $MgCl_2$ was added, and the cells were lysed by pipetting them up and down in the solution. To avoid nucleotide breakdown by the *T. brucei* cells, it was important not to include any washing step and to start the pipetting procedure immediately after the addition of the extraction solution. The lysed

cells were centrifuged at 16 000 × *g* for 1 min at 4°C, and the supernatant was transferred to a new tube and subjected to chloroform–trioctylamine extraction and WAX-SPE purification as described above. Mammalian fibroblasts were harvested at ∼70% confluence. The cells were washed with ice-cold PBS directly on the plate and placed on ice before adding 500 μl ice-cold extraction solution, which could either be 50% ACN, 80% MeOH or 10% (w/v) TCA with 15 mM $MgCl_2$ (the extraction solution is indicated in the figure legends). Immediately after the addition of extraction solution, the cells were lysed by scraping them with a cell scraper and the solution was transferred to an Eppendorf tube, centrifuged at 16 000 × *g* at 4°C, and subjected to chloroform-trioctylamine extraction (only for TCA samples) and WAX-SPE purification. Mouse embryos were snap-frozen in Eppendorf tubes in liquid nitrogen. After the addition of ice-cold 50% (v/v) ACN and glass beads, the embryos were thawed on ice and homogenized at 12 speed units for 30 s in a cold room (∼4°C) using a Bullet Blender Storm 24 instrument (Next Advance Inc., Troy, NY, USA). The resulting extracts were centrifuged at maximum speed at 4°C, and the supernatants were subjected to WAX-SPE purification. To avoid overloading of rNTPs, the samples were generally diluted before HPLC analysis. The *T. brucei*, mammalian fibroblast, and *S. cerevisiae* samples were diluted 1:1 with water before adding 10 × loading solution, whereas the more concentrated mouse embryonal extracts and *S. cerevisiae* extracts were diluted 10-fold before adding the loading solution.

DNA polymerase-dependent dNTP confirmation assay

For the dNTP confirmation assay, a sample was prepared by mixing 5 μl random decamers, 7 μl 10 × DTT-free reaction buffer (0.2 M Tris–HCl pH 7.5 and 50 mM $MgCl_2$), and 0.5 μl M13 DNA (250 μg/ml) in an Eppendorf tube. A mock sample was prepared with only 10 × reaction buffer and 7.5 μl water. The two samples were incubated at 100°C in a heating block for 7 min and chilled on ice for 15 min. Subsequently, 50 μl cell extract was added to both tubes, as well as 3.5 μl 20 μM AMP-PNP as the loading control. This loading control is optional because the cellular rNTPs can be used as a controls as well (see below). A volume of 7.5 μl Klenow exo$^-$ (5 U/μl) was added to the sample containing random decamers and M13 template, and a corresponding volume of water was used in the mock sample. The two tubes were incubated at room temperature for ∼20 h. The next day, two 3 kDa filters were washed by two 3-min centrifugations with 400 μl HPLC solution A and one 3-min centrifugation with 400 μl water at 16 000 × *g*. The remaining solution in the filter and flow-through fractions was discarded after each centrifugation by shaking the liquid off in the sink. Subsequently, the incubated samples were added to the washed filter units and collected by a 5-min centrifugation. A second 5-min centrifugation was performed with 66.5 μl water to collect the remaining sample from the filter in the flow-through. The filtrate in each tube then contained a total volume of about 140 μl. The samples were mixed with 10 × loading solution and analyzed by HPLC. Here, AMP-PNP was used as a loading control to visualize that the dilution factor during the filtration step was equal in both samples. As described in the Results and Supplementary Data, the rNTP peaks can be used for the same purpose, but this is less convenient for visualization because rNTPs cannot be shown at the same scale as the dNTPs. The exclusion of DTT in the reaction buffer and in the washing of the filters was necessary to remove unwanted peaks resulting from the DTT and from contaminants on the filter. The dNTP confirmation is primarily needed for new types of samples as described in the results section.

Calculations of cellular nucleotide pools

The HPLC results were compared to a nucleotide standard containing 1 μM of ADP, rNTPs and dNTPs. Peak areas were used for the quantification of ADP and rNTPs, whereas peak heights were used for the dNTPs. However, because of the overlap between GTP and UTP, we recommend using the peak height for the smallest of the two peaks in cell extracts where there is more than a 2-fold area difference between them. The amount in nmol/sample was calculated by multiplying the obtained nucleotide concentrations by the dilution factor and the volume in ml of the SPE-purified sample.

Statistical analyses

The collection and analysis of dNTPs and rNTPs from *S. cerevisiae* were performed in three independent experiments with standard deviations shown by error bars. The figures and chromatograms were plotted with the GraphPad Prism 8.0.2 software (GraphPad Software Inc., San Diego, CA, USA). The chromatograms were recorded by the ChromPerfect software (Justice Innovations Inc., Denville, NJ, USA), and the data points were exported to GraphPad Prism, which was more flexible for labeling peaks and made it possible to also use logarithmic axes when desired.

RESULTS

Limitations of gradient reverse phase HPLC conditions for nucleotide analysis

Previous protocols for reverse phase HPLC analysis of nucleotides are in most cases based on TBA for ion pairing, with the elution driven by a phosphate gradient in combination with low concentrations of MeOH. We found that gradient reverse phase HPLC methods were useful for separating the most abundant nucleotides and nucleotide-conjugated sugars in the cell (Figure 1A). However, a rising baseline from impurities in the phosphate salts made it difficult to quantify the much less abundant dNTPs (Figure 1B). Another issue was multiple minor peaks that could interfere with the analysis. The three most abundant unknown peaks are indicated as N_x, N_y and N_z in the figure. To solve the problem with the rising baseline, we switched to isocratic HPLC instead of using gradient-based elution. In parallel with the isocratic HPLC method development, which is described in the next section, we also analyzed other peaks observed in Figure 1. NAD^+, rNMPs/dNMPs and the indicated UDP/GDP-conjugated sugars eluted much earlier than the rNTPs and dNTPs and were not of a concern for development of the isocratic HPLC. The N_x, N_y and

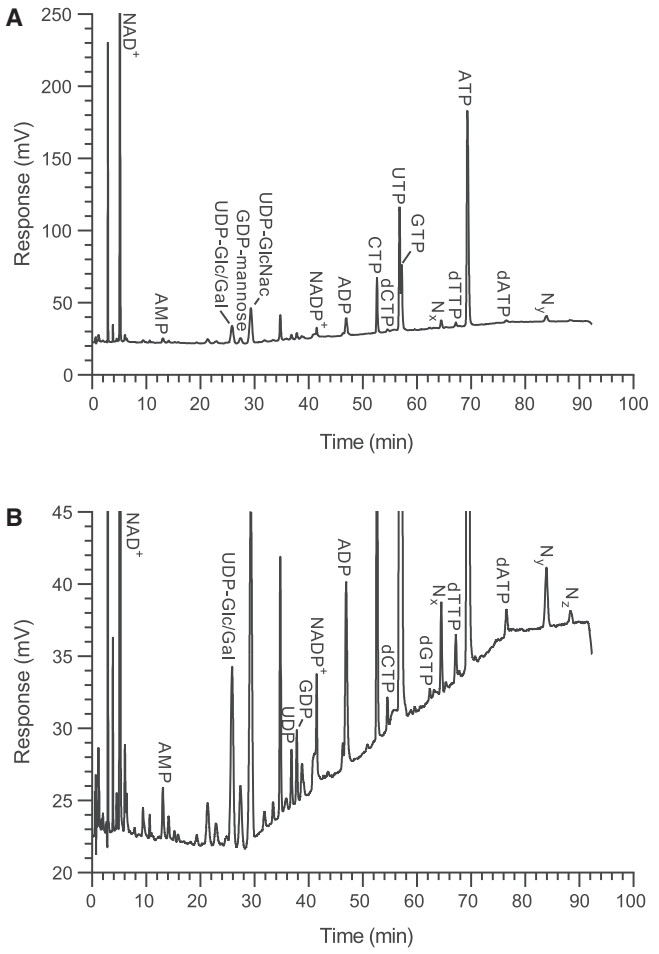

Figure 1. Analysis of nucleotides in a *S. cerevisiae* TCA extract using gradient HPLC on a 100 mm × 2.1 mm ACE Excel 2 C18 column. (**A**, **B**) The chromatogram in B is from the same experiment as in A but shown at a higher magnification to visualize the dNTPs. The KP_i gradient started with an isocratic step from 0 to 25 min with 7% MeOH, 0.7 g/l TBA-Br and 0.92 g/l KP_i pH 5.6, followed by a gradient between 25 and 75 min up to 7% MeOH, 0.7 g/l TBA-Br and 13.8 g/l KP_i pH 5.6, and a final isocratic step between 75 and 90 min before returning to the initial conditions. The column temperature was 40°C, the flowrate 0.4 ml/min, the UV wavelength 270 nm, and the loop size 5 μl. The wash step with NH_3-containing MeOH was omitted from the WAX-SPE purification step in this case to also show NMPs and UDP-conjugated sugars that are not normally efficiently recovered in the SPE procedure.

N_z peaks were concluded to be acid degradation products of NADPH because they also appeared with TCA-treated NADPH solutions (Supplementary Figure S1A). The N_x peak had a retention time indicating 2′-phospho-ADP ribose (PADPR) (Supplementary Figure S1B), which is a known acid degradation product of NADPH (23,24), whereas N_y and N_z are still unknown.

The *S. cerevisiae* extracts also contained a broad peak denoted b_1, which had a wide-ranging absorption profile (Supplementary Figure S2A). The absorption at long wavelengths was advantageous for the development of a subtraction procedure in which removing 1.8 times the recorded signal at 310 nm from the 270 nm-chromatogram almost entirely eliminated the b_1 peak and a second smaller broad peak termed b_2 (Supplementary Figure S2B). Most cell types do not contain these peaks, but in *S. cerevisiae* and other species where they exist this procedure is an efficient way to eliminate them. An alternative strategy is to reduce the sample loop volume. By using a five times more concentrated sample and a 20 μl sample loop instead of 100 μl on a 4.6 mm × 150 mm column, the b_1 and b_2 peaks became much smaller (Supplementary Figure S3A). The b_1 and b_2 peaks were more prominent if the mobile phase solution A (containing KP_i) had been stored for several months, indicating that these peaks originated from interactions of the cell extract with the mobile phase impurities rather than coming from the sample itself (Supplementary Figure S3B). For the remaining experiments, we have been careful to not use KP_i solutions older than one month, but without subtraction procedure to be able to show in which type of analyses the b_1 and b_2 peaks appear.

Complementary studies on how the mobile phase affects peak positions showed that b_1 and b_2 shifted to the left relative to rNTPs/dNTPs at increased KP_i concentration, whereas N_y and N_z were always the last eluting peaks under these conditions and did not normally influence the nucleotide analysis (Supplementary Figure S4). rNDPs, dNDPs, PADPR and UDP-glucuronic acid (UDP-GlcA) were included in our nucleotide standards for further optimization of the chromatography conditions. UDP-GlcA contains additional negative charges relative to other UDP-conjugated sugars and elutes in the rNTP-dNTP region in reverse phase HPLC chromatograms with TBA as the ion pairing agent (12). This nucleotide-conjugated sugar is not present in *S. cerevisiae* but is common in animals, plants, and many other species, including both eukaryotes and prokaryotes (25–28).

Developing the isocratic HPLC conditions for nucleotide analysis

To solve the problem with the rising baseline using gradients, we switched to isocratic HPLC, which made it possible to resolve ADP and rNTPs from cell extracts within a reasonable time when using 5 cm ACE C18-AR and C18-PFP columns (Supplementary Figure S5). However, most dNTP peaks except for dTTP were below the detection limit under these conditions and were not properly resolved from other small peaks when increasing the amount of sample. It was therefore necessary to use a longer column (4.6 mm × 150 mm Sunshell C18-WP-2.6 μm column), but then the analysis took nearly 2 h (Figure 2A). The elution order of different rNTPs and dNTPs was the same as with the ACE Excel 2 C18 column used in Figure 1, and the resolution for a given column length was also comparable. However, the lower backpressure of the solid-core Sunshell material made it the preferred choice for further studies.

A crucial finding was that by switching from MeOH to ACN in the mobile phase, it became possible to separate nucleoside di- and triphosphates within a three times shorter analysis time and with much higher sensitivity (Figure 2B). A main reason for why gradient methods have been preferred in the past is that the rNDPs, dNDPs, and most nucleotide-conjugated sugars elute in the initial low-phosphate conditions and do not interfere with the rNTPs

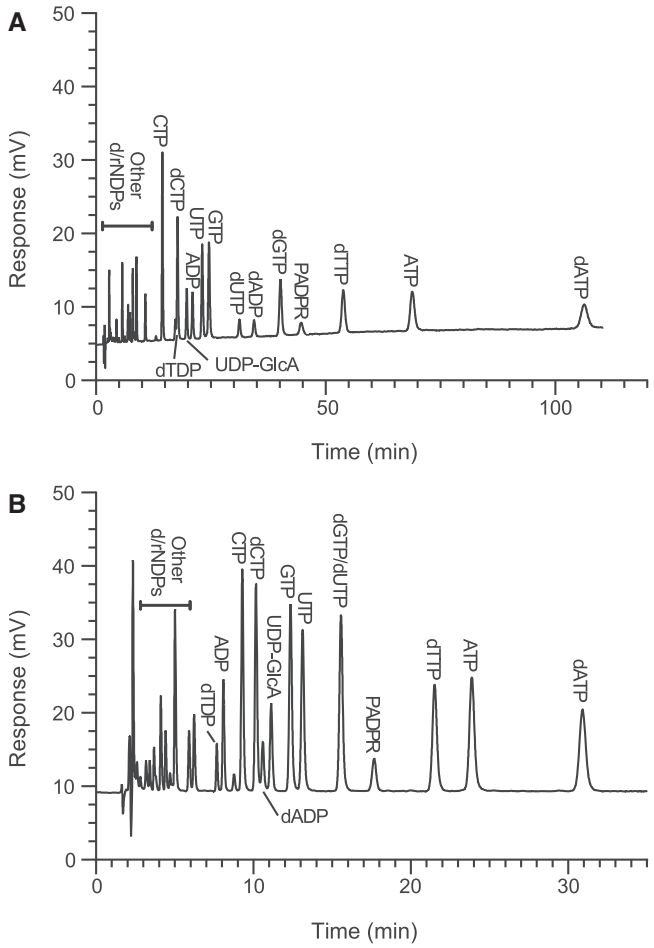

Figure 2. HPLC chromatograms from nucleotide standards with MeOH or ACN as the organic modifier in the mobile phase. (**A**) Analysis of a nucleotide standard on a 150 mm × 4.6 mm Sunshell C18-WP column with a mobile phase containing 7% MeOH, 0.7 g/l TBA-Br, and 9.2 g/l KP_i pH 5.6. (**B**) Similar analysis as in A but with 7% ACN instead of MeOH. The nucleotide standard contained 0.25 μM of most rNDPs-dNDPs (except ADP that was 0.4 μM), 0.5 μM UDP-GlcA and PADPR, and 1 μM of most rNTPs-dNTPs (except dUTP, which was 0.25 μM). The HPLC experiments were performed with ambient column temperature, 270 nm wavelength, and 50 μl loop volume. Note that the flow rate was 0.8 ml/min, which gave longer retention times than the 1.2 ml/min used in our final HPLC protocols.

and dNTPs coming later in the phosphate gradient. Replacing MeOH with ACN gave a similar effect under isocratic conditions, and all diphosphates except dADP eluted before the triphosphates. The elution order of diphosphates was the same as that of triphosphates with the last three being dTDP, ADP and dADP. A notable difference with ACN compared to MeOH was that the purine nucleotides shifted to the left relative to the pyrimidine nucleotides leading to earlier elution of the last nucleotides, ATP and dATP, which contributed to the much shorter overall retention time. Another consequence of the shorter purine retention times was that the elution order of GTP and UTP were opposite with ACN compared to MeOH.

To get a better understanding of how the mobile phase composition affects the separation of the nucleotides and to find a way to separate dUTP and dGTP, we tested the effects of pH, KP_i concentration, ACN concentration, and temperature on nucleotide separation. All of these factors had a general effect where increasing pH, temperature, KP_i concentration, and ACN concentration gave shorter retention times (Supplementary Figure S6), but the strength of this effect was dependent on the type of nucleotide. By replotting the capacity factors (retention time minus void time) of all nucleotides relative to those of UTP, it was possible to get information about how the nucleotide peaks shift relative to each other when changing mobile phase conditions. Supplementary Figures S7–S8 show a more extensive analysis of these results, and the most important findings for the development of our final protocol were the following:

- pH – The main reason why we chose a pH of 5.6 was to get good separation of dCTP from CTP. In addition, the pH had a major impact on the positions of diphosphates and UDP-GlcA relative to the triphosphates.
- ACN concentration – Lowering the ACN concentration to 5.86% enabled the separation of dGTP and dUTP. A general trend when decreasing the ACN concentration was a more pronounced increase in the retention times of purines relative to pyrimidines.
- KPi concentration – This is a useful final parameter to fine-tune the positions of ADP, dADP and unknown peaks (described below) without affecting the already optimized positions of rNTPs and dNTPs.

The outcome of the chromatographic condition optimization was an HPLC method termed the High-Resolution Protocol (Table 1). Figure 3A shows the HPLC analysis of a sample from a mouse embryo extracted with 50% ACN using this HPLC protocol. All dNTPs were clearly resolved from the rNTPs. Two other peaks, named c and g due to their proximity to dCTP and dGTP, respectively, were also present. Supplementary Figure S9A–C describes the chromatographic behavior of these peaks. The rationale behind selecting an embryonal extract for these studies was that it represents an average sampling of the cell types in the body and therefore gives better coverage of additional peaks to consider when optimizing an HPLC protocol for general use. The dUTP levels were undetectable in the embryonal extract, which is in line with our previous observations in *S. cerevisiae* that dUTP is only detectable if enzymes involved in its metabolism are mutated (29). We also created a second HPLC protocol termed the Fast Protocol. In this protocol, the column temperature is 30°C instead of ambient and the KP_i concentration is increased. This makes the separation faster, but the dUTP and dGTP peaks merge and the method is also less suitable for samples prepared with TCA as the extraction solvent (described below). Figure 3B shows the HPLC chromatograms from mouse fibroblasts sampled with different extraction solutions using the Fast Protocol. Generally, the organic extraction solutions gave cleaner chromatograms, whereas the TCA extract analysis showed a series of extra peaks, including the NADPH breakdown products PADPR, N_y, and N_z mentioned above and an impurity from the TCA solution called t. The t-peak did not interfere with the analysis

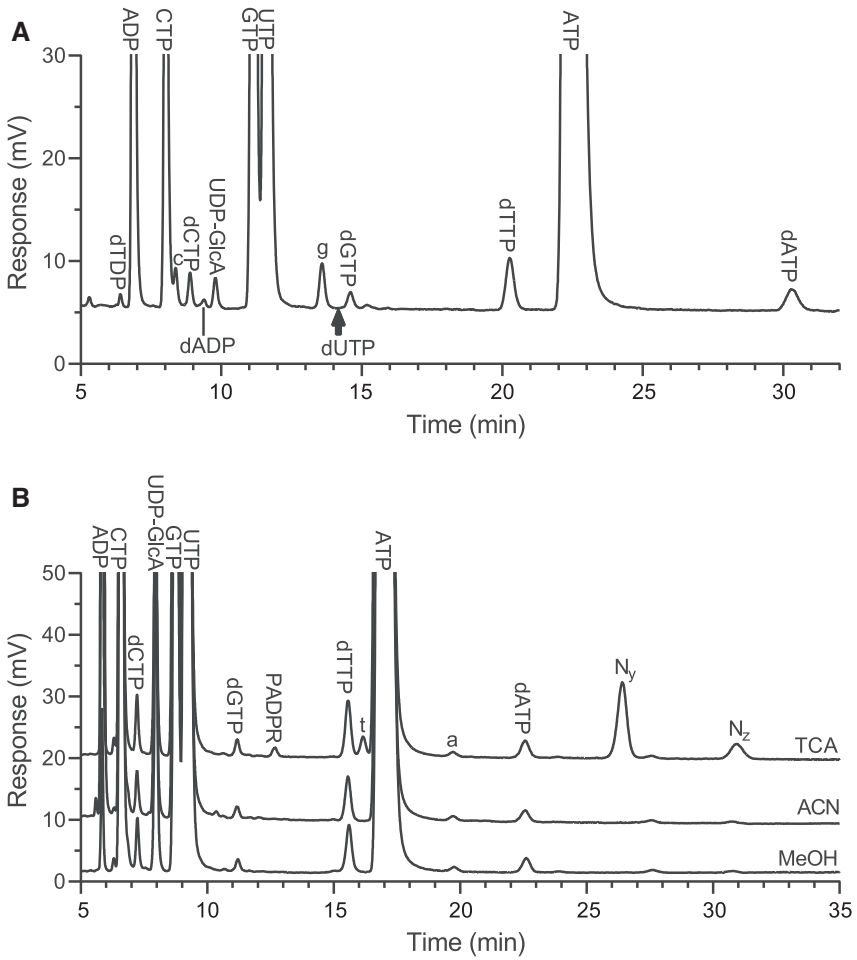

Figure 3. HPLC analyses of extracts from mouse embryos and Balb/3T3 cells. (**A**) Nucleotide analysis using the high-resolution protocol on a sample prepared from mouse embryos extracted with 50% ACN. (**B**) Nucleotide analysis using the fast protocol on samples prepared from Balb/3T3 fibroblasts extracted with 10% TCA (+ 15 mM $MgCl_2$), 50% ACN, or 80% MeOH. Peaks c, g and a are unknown components from the extracts, and t is from the TCA solution.

using the High-Resolution Protocol where it eluted a comfortable distance before dTTP (Supplementary Figure S10A). In contrast, it eluted very closely after dTTP when using the Fast Protocol (Figure 3B). If desired, it was possible to eliminate this peak by replacing TCA with TFA (Supplementary Figure S10B). The cell extracts also contained a well-resolved minor peak, a, which did not interfere with the analysis (Figure 3B). The t and a peaks were named by the dNTP they were closest to following the same naming system as for the c and g peaks.

Other potential sources of peaks are the mobile phase and the solutions used in the WAX-SPE purification. In our case, the SPE solutions did not contain any components in the rNTP-dNTP region of the chromatogram, and the mobile phase contributed with only two minor peaks named m^- and m^+ eluting just before ADP and CTP, respectively (Supplementary Figure S11). The chromatographic properties of the c, g, t, m^- and m^+ peaks are described in the Supplementary Data (Figures S9-11). The retention times of all of these peaks were much less sensitive to changes in mobile phase KP_i concentration than the rNTP and dNTP peaks, which made it possible to fine-tune the conditions to separate the nucleotides from the other compounds in both HPLC protocols. Finally, we analyzed the loading capacity of the column and the influence of the flow rate on the resolution (Supplementary Figure S12). The flow rate selected for both protocols was 1.2 ml/min, which is higher than optimal for the resolution but gives significantly shortened analysis times with a backpressure still low enough to work on most HPLC systems (300–320 bar).

Development of the TCA extraction method

A commonly used solution for cellular nucleotide extractions is 10–12% (w/v) TCA supplemented with 15 mM $MgCl_2$ (24). The $MgCl_2$ is required to minimize the loss of nucleotides in the subsequent extraction step with a mixture of Freon (1,1,2-trifluoro-2,2,1-trichloroethane) and trioctylamine. Because the use of Freon is restricted, a new extraction method based on chloroform-trioctylamine was evaluated. The new extraction solution could efficiently remove the acid resulting in a pH of 5 or higher and gave nucleotide recoveries of 84–91%, which was nearly as high as with Freon-trioctylamine (Supplementary Table S1).

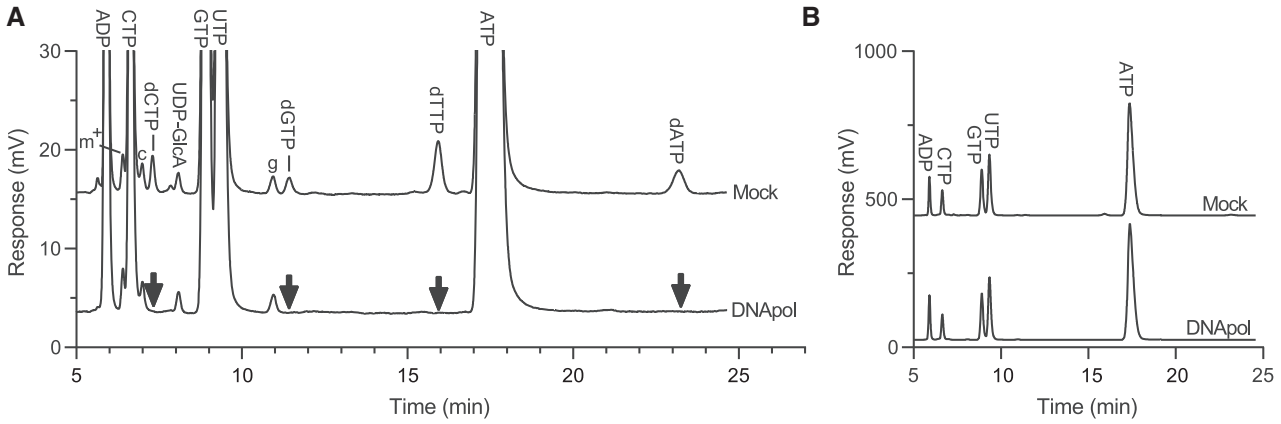

Figure 4. HPLC analysis of an extract from an 11.5-day-old C57BL/6 mouse embryo using the dNTP confirmation assay. (**A**) The two chromatograms show a mock-treated sample and a sample treated with DNA polymerization reagents (DNApol). M13 DNA, primers and DNA polymerase were present only in the DNApol sample, but the treatments were otherwise identical. The arrows in the bottom chromatogram show the specific removal of dNTPs. Peaks c and g are unknown components in the cellular extracts. (**B**) The same chromatograms as in A but shown at a lower magnification to visualize the rNTPs used as internal loading controls. The Fast Protocol was used for the HPLC analysis.

Development of a dNTP confirmation assay for impurity control

An important aspect for a reliable HPLC method is to ensure that there are no other compounds co-eluting with the peaks of interest. This is generally no problem for rNTPs, but because dNTPs are far less abundant their analysis can be obstructed by co-eluting peaks. Because the number of additional peaks varies depending on the extraction solution, cell type, purity of the reagents, and mechanical forces during extraction, we developed an assay for the selective removal of dNTPs. It is thereby possible to confirm that the peaks represent pure dNTPs with no UV-absorbing compounds eluting at the same position. For each assay, we prepared two samples. One sample contained components required for DNA polymerization as described in the Materials and Methods, whereas the other sample lacked them. After a 20-h incubation period and subsequent filtration to remove enzymes and DNA, the samples were analyzed by HPLC. This procedure worked with all extracts studied here, including mouse embryos (Figure 4A), Balb/3T3 fibroblasts, *T. brucei*, and *S. cerevisiae* (Supplementary Figure S13). The rNTPs are not affected by this procedure, which make them suitable as controls to ensure that the sample loading is equal in the two chromatograms (Figure 4B). An alternative to plot a separate graph with rNTPs, is to use AMP-PNP as loading control as shown in Supplementary Figure S13.

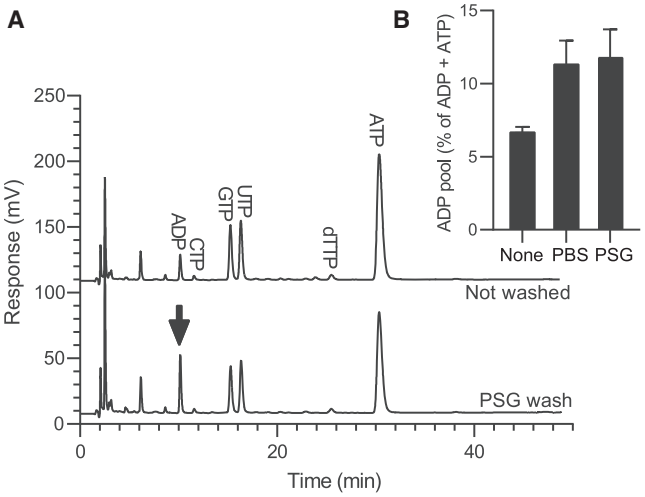

Figure 5. The effect of cell washes on the ADP pool. (**A**) HPLC chromatograms showing two *T. brucei* samples from the same batch where only the second was exposed to a wash step with PSG (PBS pH 7.4 supplemented with 1% w/v glucose). The arrow highlights the increase in ADP that occurs during the wash. (**B**) The relative ADP pools expressed as a percent of the total ADP + ATP pool in *T. brucei* cells using different washing solutions. The cells were extracted with TCA and analyzed with the High-Resolution Protocol but with a flow rate of 0.9 ml/min.

Cell washes

Cell culture media can yield extra peaks in HPLC, and it is therefore common to wash the cells prior to the extraction of nucleotides. The media used for *T. brucei* and mammalian cells were free from extra peaks (Supplementary Figure S14A), whereas the YPD used for *S. cerevisiae* cultures gave a whole range of extra peaks that could only be partially removed by the WAX-SPE purification step (Supplementary Figure S14B). Further analysis showed that the peaks came primarily from the yeast extract component of the growth medium and to a lesser extent from peptone (Supplementary Figure S14C). The peaks coming from the growth medium were removed by washing the cells twice with a glucose-containing PBS solution before adding the extraction solution to create chromatograms free from media-derived peaks (Supplementary Figure S13C, D). However, it is not always beneficial to use a washing step, as shown for *T. brucei* where even a short washing step is enough to cause a decreased energy charge (ATP:ADP ratio), and this is also the case if glucose is included in the washing solution (Figure 5). This experiment illustrates the benefit of being able to measure ADP, which is less

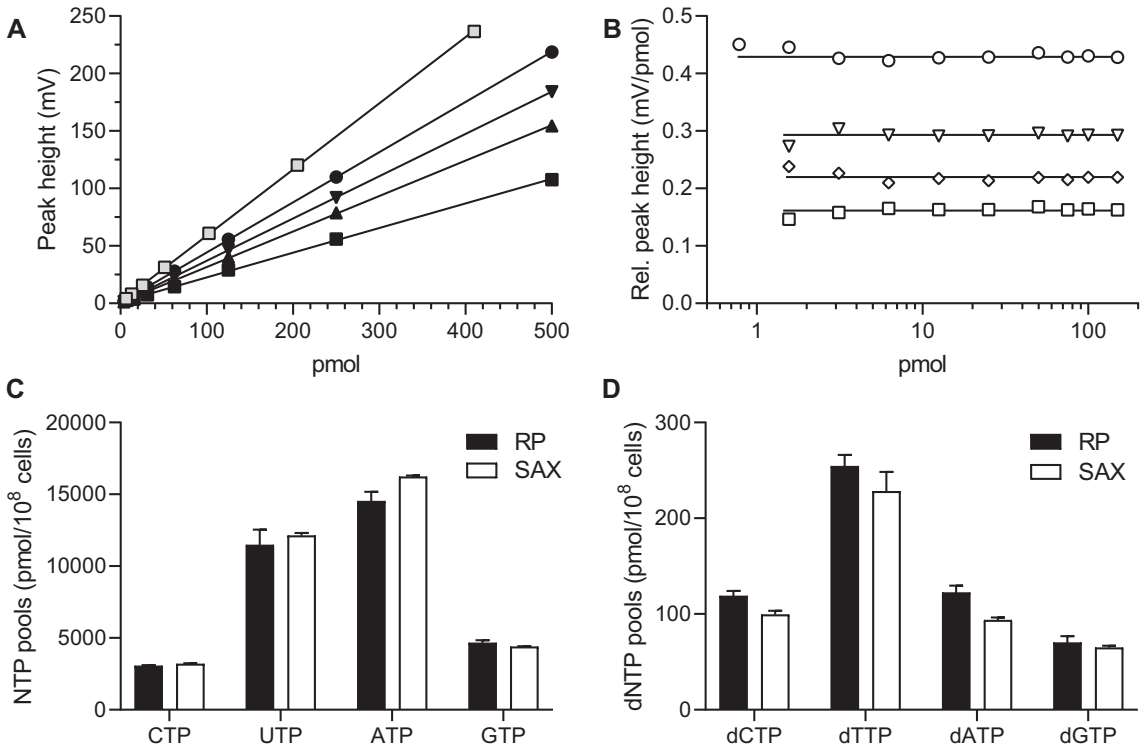

Figure 6. Nucleotide quantification analysis. (**A**) Peak height as a function of the amount in pmol for ADP (□), CTP (●), UTP (▲), GTP (▼) and ATP (■). (**B**) Relative peak heights of dNTPs as a function of the amount of dCTP (○), dGTP (▽), dTTP (◊) and dATP (□). Horizontal lines correspond to linearity in the type of plot shown in B. (**C**) rNTP quantification from *S. cerevisiae* cells using the new reverse phase (RP) HPLC method (Fast Protocol) compared with the previously used strong anion exchange (SAX) HPLC method. (**D**) Quantification of dNTPs from *S. cerevisiae* cells using the RP and SAX HPLC methods. The RP method includes a WAX-SPE purification step, and the SAX protocol includes a boronate purification step, but only for the dNTPs.

abundant than ATP and thereby a more sensitive indicator of disturbed metabolism. It is sufficient that only 5–10% of the ATP is degraded to see a clear effect on the ADP pool (Figure 5B). We conclude therefore that it is important to monitor the effects of the washing steps on the energy charge by analyzing the ATP to ADP ratio and that it is only with broth-type media (containing yeast extract and peptone) that it is necessary to include a cell wash.

Linear range and sensitivity of the HPLC analysis

Plotting HPLC peak heights or areas as a function of concentration for the rNTPs or dNTPs resulted in straight lines, with R^2 values of 0.999 or higher (exemplified in Figure 6A). However, to get a better insight into how accurate the rNTP-dNTP quantification is in a situation where the column is overloaded with rNTPs, which is often the case with cellular samples, we prepared a dilution series starting from a stock solution with 60 μM ATP, 15 μM of other rNTPs, 1.5 μM dNTPs and 24.6 μM ADP. To monitor the linearity over a wide range, the results were plotted as relative peak heights (i.e. per pmol) using a logarithmic spacing on the x-axis. The horizontal lines in Figure 6B show that the quantification of dNTPs is linear all the way up to the highest amount tested. Thus, the dNTP peak heights are linear also in a background of much higher rNTPs. The corresponding rNTP data were nearly linear up to approximately 500 pmol, with an increasing deviation at higher amounts (Supplementary Figure S15A). For the ADP and rNTP peaks it was therefore preferable to use peak areas, which were linear over the whole range tested (Supplementary Figure S15B). The dNTP analysis showed a high sensitivity with accurate measurements of dCTP down to ∼0.8 pmol, and other dNTPs to ∼1.6 pmol, which is comparable to mass spectrometry-dependent measurements reporting a detection limit just below 1 pmol (5). Finally, we also compared our newly developed reverse phase HPLC method (Fast Protocol) with the previously used anion exchange HPLC method for nucleotide quantification from *S. cerevisiae* cells (Figure 6C, D). The reverse phase method includes the WAX-SPE step prior to the simultaneous measurement of rNTPs and dNTPs, whereas the anion exchange method includes a boronate purification step for dNTP analysis but not for rNTPs. The anion exchange method gave slightly lower dNTP values, which could possibly be due to losses during the additional boronate step. The purpose of the nucleotide analyses is generally to detect unbalanced dNTP pools or gross changes in their total level, and the small difference between RP and SAX can be concluded to be well within the acceptable range.

DISCUSSION

A large variation in results from dNTP pool measurements between different laboratories has been a problem for

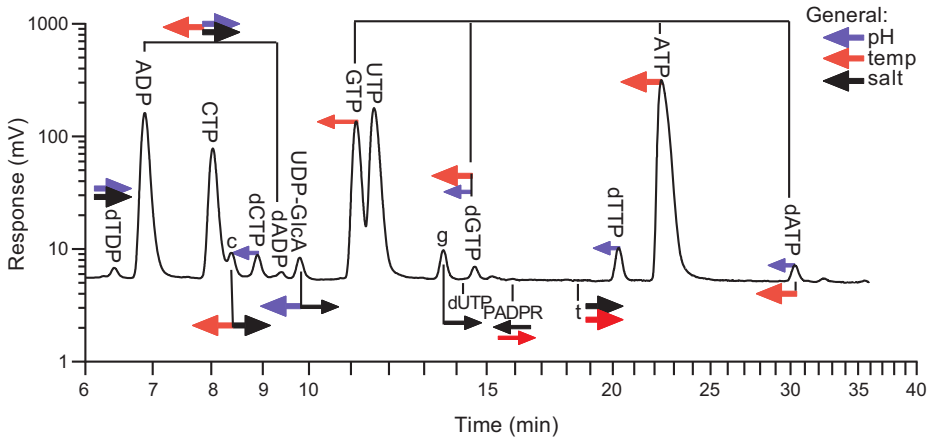

Figure 7. HPLC analysis of a mouse embryonal ACN extract using the high-resolution protocol with arrows indicating how different parameters affect the movement of peaks. The arrows in the chromatogram indicate how different peaks move in relation to the UTP peak when increasing the pH, temperature, or salt concentration (KP_i), with arrow sizes related to the strength of the effect. The four purine triphosphates and two purine diphosphates are grouped together to highlight that that they are affected in a common way. Logarithmically spaced units on both axes prevent crowding in the beginning of the chromatogram and make it possible to show rNTPs and dNTPs in the same graph despite the large differences in retention time and quantity. Note that the logarithmic ordinate will emphasize the base of large peaks, which gives a false impression that the overlap between GTP and UTP is larger than it is. This peak distortion only affects peaks that are considerably larger than the introduced baseline offset (5 mV) needed for the creation of logarithmic plots. The two impurity peaks N_y and N_z are not visible in the plot because they elute later.

decades (6). At least during the setup stage, it is advantageous to use a method that measures not just the dNTPs, but also other metabolites that could be used as internal controls, and in that case the HPLC-based methods are superior to the DNA polymerase-dependent techniques. The dNTP pools vary depending on the cell growth phase, with stationary cells having much lower dNTPs than logarithmically growing cells (5). In contrast, rNTP pools are much less variable, which makes it easier to compare the extraction efficiency between different laboratories (2,18). With the ability to also detect ADP, we have an additional tool to measure the quality of cell extracts. Figure 5 shows how the ADP measurement helped us to improve the protocol for extraction of *T. brucei* cells to minimize the effects on the ATP:ADP ratio. Because all rNTPs and dNTPs are metabolically linked to each other to varying degrees via NDP kinase and other nucleotide-dependent enzymes, it is important to minimize excessive nucleotide degradation. In the *T. brucei* case, the ATP degradation was modest with ATP going from 93% to 87% of the total ATP + ADP pool yielding a very small change in the phosphorylating capacity of other nucleotides. However, our experience is that other parameters such as differences in extraction speed or handling techniques can sometimes lead to much higher ATP degradation. With the measurements of ADP, we now have a tool to immediately identify the problem and correct the extraction technique if needed. In the example with *T. brucei* cells, the modest decrease in ATP was accompanied by a nearly doubled ADP level from 7% to 12% of the total ADP + ATP pool and was therefore easily detectable. It is difficult to know what the ATP:ADP ratio is in untreated cells, but in our experience dNTPs and rNTPs are not significantly converted into their diphosphate forms as long as the ATP:ADP ratio is ∼10 or higher. This corresponds to 9 out of 10 adenine ribonucleotides being in the ATP form, which in turn controls the phosphorylation status of other rNTPs and dNTPs.

Two findings were important for the development of ion-pair C18 chromatography for the analysis of cellular dNTP pools. The first was to switch to isocratic HPLC to get a straight baseline. It was then crucial to replace MeOH with ACN in the mobile phase to enable separation within a reasonable time frame. The second finding was the development of the dNTP confirmation assay to rule out that no peaks with the same retention time as the dNTPs disturbed the analysis. Co-eluting peaks could possibly explain the extreme variation in dNTP pools between different mammalian cell lines in previous attempts to measure rNTPs and dNTPs at the same time (17). Whenever such an overlap is detected, it is an advantage to have an HPLC method with the built-in flexibility to be able to shift the peaks in the chromatogram in a predictable manner. From the analysis of how the mobile phase composition influences the retention time of rNDPs, rNTPs, dNTPs, and other nucleotide-derived cellular metabolites, some general conclusions can be drawn (Figure 7). There was a general shift of peaks to the left with higher temperature, organic content, or KP_i concentration. This is not surprising because ACN and high temperatures prevent interactions with the reverse phase material, whereas KP_i and other salts inhibit the binding of the nucleotides to the ion pairing agent. However, relative movements of the peaks are also important when optimizing separation, and Figure 7 shows the movement of the peaks relative to UTP, which was selected as the reference point. CTP always followed UTP and therefore had a fixed position relative to UTP, whereas the purines shifted to the left with higher temperature or ACN concentration. The dNTPs followed the corresponding rNTPs well except for a slight shift to the left at higher pH, whereas the diphosphates (rNDPs/dNDPs)

shifted to the right with higher salt concentration or pH. From a practical viewpoint, 10–15 min is generally a sufficient equilibration time for changes in temperature or salt concentrations, whereas changes in the ACN concentration and especially pH require longer equilibration times. It is therefore rather quick to switch between the Fast and High-Resolution Protocols, which only differ by temperature and KP_i concentration. The experiment in Figure 7 was at ambient temperature using the High-Resolution Protocol, and the lower temperature made it possible to separate dGTP from dUTP. The chromatogram in Figure 7 has logarithmic axes to be able to visualize the rNTPs and dNTPs in a single chromatogram and with arrows showing the movement of all peaks under different conditions. The kind of scheme shown in Figure 7 was important for the development of our two HPLC protocols and is also convenient for the development of new ones if additional peaks are encountered in cell extracts. Supplementary Figure S16 gives a summary of logarithmic chromatograms with the two HPLC protocols using different cell types and extraction conditions.

Figure 7 also includes the movements of four categories of additional peaks in the extracts. The first category is the TCA-specific peaks, including the t-peak and the three NADPH degradation products PADPR, N_x and N_y. Only the t-peak and PADPR are shown in Figure 7 because N_x and N_y elute later. The t-peak is an impurity in most TCA sources and disappears if using TFA instead. The NADPH-derived peaks were never of any problem for nucleotide analysis, and the only disadvantage with them is that the N_x and N_y peaks elute later than the rNTPs and dNTPs and thereby increase the total analysis time. The second category contains peaks coming from the mobile phase in the injection process (m^+, m^-, b_1 and b_2). The m-peaks were very small and did not interfere with dNTP analysis. However, they may vary depending on the mobile phase and HPLC system, and it is therefore good to include a mock analysis without cell extract to know their position before the analysis of real samples. The b_1 and b_2 peaks were very broad and dependent on both the type of extract and the source of phosphate in the mobile phase, indicating that they most likely come from the influence of unknown components in cell extracts on the retention of mobile-phase phosphate impurities. Two strategies made it possible to minimize the influence of the b_1 and b_2 peaks in the chromatograms. The most powerful approach was a UV subtraction procedure that almost completely removed the two peaks, but a simpler option was to use a smaller sample loop and a more concentrated sample instead. The third category is cell type-specific peaks. Most of them were very small except for UDP-GlcA, dADP, and a few unknown peaks named with a one letter abbreviation system after the dNTP they were closest to (c.g. t, and a). The fourth category is peaks coming from the culture medium. No such peaks were observed when using tissue culture media (DMEM and HMI-9), whereas broth-type media containing yeast extract and peptone generated a whole range of peaks possibly coming from partially degraded proteins and nucleic acids. Although cell washes normally remove these peaks, it is important to verify that the energy charge in the cells remains intact during the washes by measuring the ATP to ADP ratio (Figure 5). An alternative option can be to develop a wash-free protocol by replacing the yeast extract and peptone with free amino acids and other defined media components.

A major challenge in nucleotide analysis has been to study cells treated with the deoxynucleoside analogues used in anticancer and antiviral therapy. In this case, current methods often fail because the triphosphate forms of the analogues disturb DNA synthesis in enzyme-based methods and are often difficult to separate from natural rNTPs and dNTPs in anion exchange HPLC methods. In this case, we see a great advantage with the new reverse phase-ion pair method presented here that provides sufficient space between the peaks and has the flexibility shown in Figure 7 for repositioning the peaks in cases of overlaps. An additional advantage is the low detection limit (~1 pmol), which is by far the highest sensitivity achieved for nucleotide analysis with UV-based HPLC methods and is comparable to mass spectrometry-based detection. We therefore believe that it has the potential to become a major method for future nucleotide analysis.

DATA AVAILABILITY

All data are available in the main text or in the Supplementary data.

SUPPLEMENTARY DATA

Supplementary Data are available at NAR Online.

ACKNOWLEDGEMENTS

We would like to thank Daniel Wang Steck and Stephane Kamte for their contribution in the development of the cell washes and Cecilia Baldassarri, Pierluigi Felicioni, Elisa Marangoni and Maasho Negash for their work on *T. brucei* extraction.

FUNDING

Swedish Research Council [2019-01242 to A.H. and 2018-02579 to A.C.]; Swedish Cancer Society [19 0402 Pj to A.C.]. Funding for open access charge: Swedish Research Council (Vetenskapsrådet - VR) [2019-01242].
Conflict of interest statement. None declared.

REFERENCES

1. Kumar,D., Abdulovic,A.L., Viberg,J., Nilsson,A.K., Kunkel,T.A. and Chabes,A. (2011) Mechanisms of mutagenesis in vivo due to imbalanced dNTP pools. *Nucleic Acids Res.*, **39**, 1360–1371.
2. Chabes,A., Georgieva,B., Domkin,V., Zhao,X., Rothstein,R. and Thelander,L. (2003) Survival of DNA damage in yeast directly depends on increased dNTP levels allowed by relaxed feedback inhibition of ribonucleotide reductase. *Cell*, **112**, 391–401.
3. Mathews,C.K. (2015) Deoxyribonucleotide metabolism, mutagenesis and cancer. *Nat. Rev. Cancer*, **15**, 528–539.
4. Kunz,B.A., Kohalmi,S.E., Kunkel,T.A., Mathews,C.K., McIntosh,E.M. and Reidy,J.A. (1994) International Commission for Protection Against Environmental Mutagens and Carcinogens. Deoxyribonucleoside triphosphate levels: a critical factor in the maintenance of genetic stability. *Mutat. Res.*, **318**, 1–64.

5. Kong,Z., Jia,S., Chabes,A.L., Appelblad,P., Lundmark,R., Moritz,T. and Chabes,A. (2018) Simultaneous determination of ribonucleoside and deoxyribonucleoside triphosphates in biological samples by hydrophilic interaction liquid chromatography coupled with tandem mass spectrometry. *Nucleic Acids Res.*, **46**, e66.
6. Traut,T.W. (1994) Physiological concentrations of purines and pyrimidines. *Mol. Cell. Biochem.*, **140**, 1–22.
7. Wilson,P.M., Labonte,M.J., Russell,J., Louie,S., Ghobrial,A.A. and Ladner,R.D. (2011) A novel fluorescence-based assay for the rapid detection and quantification of cellular deoxyribonucleoside triphosphates. *Nucleic Acids Res.*, **39**, e112.
8. Hollenbaugh,J.A. and Kim,B. (2016) HIV-1 reverse transcriptase-based assay to determine cellular dNTP concentrations. *Methods Mol. Biol.*, **1354**, 61–70.
9. Ferraro,P., Franzolin,E., Pontarin,G., Reichard,P. and Bianchi,V. (2010) Quantitation of cellular deoxynucleoside triphosphates. *Nucleic Acids Res.*, **38**, e85.
10. Nick McElhinny,S.A., Watts,B.E., Kumar,D., Watt,D.L., Lundstrom,E.B., Burgers,P.M., Johansson,E., Chabes,A. and Kunkel,T.A. (2010) Abundant ribonucleotide incorporation into DNA by yeast replicative polymerases. *Proc. Natl. Acad. Sci. U.S.A.*, **107**, 4949–4954.
11. Sharma,S., Koolmeister,C., Tran,P., Nilsson,A.K., Larsson,N.G. and Chabes,A. (2020) Proofreading deficiency in mitochondrial DNA polymerase does not affect total dNTP pools in mouse embryos. *Nat Metab*, **2**, 673–675.
12. Qin,X. and Wang,X. (2018) Quantification of nucleotides and their sugar conjugates in biological samples: purposes, instruments and applications. *J. Pharm. Biomed. Anal.*, **158**, 280–287.
13. Shewach,D.S. (1992) Quantitation of deoxyribonucleoside 5′-triphosphates by a sequential boronate and anion-exchange high-pressure liquid chromatographic procedure. *Anal. Biochem.*, **206**, 178–182.
14. Garrett,C. and Santi,D.V. (1979) A rapid and sensitive high pressure liquid chromatography assay for deoxyribonucleoside triphosphates in cell extracts. *Anal. Biochem.*, **99**, 268–273.
15. Decosterd,L.A., Cottin,E., Chen,X., Lejeune,F., Mirimanoff,R.O., Biollaz,J. and Coucke,P.A. (1999) Simultaneous determination of deoxyribonucleoside in the presence of ribonucleoside triphosphates in human carcinoma cells by high-performance liquid chromatography. *Anal. Biochem.*, **270**, 59–68.
16. Di Pierro,D., Tavazzi,B., Perno,C.F., Bartolini,M., Balestra,E., Calio,R., Giardina,B. and Lazzarino,G. (1995) An ion-pairing high-performance liquid chromatographic method for the direct simultaneous determination of nucleotides, deoxynucleotides, nicotinic coenzymes, oxypurines, nucleosides, and bases in perchloric acid cell extracts. *Anal. Biochem.*, **231**, 407–412.
17. Huang,D., Zhang,Y. and Chen,X. (2003) Analysis of intracellular nucleoside triphosphate levels in normal and tumor cell lines by high-performance liquid chromatography. *J. Chromatogr. B Analyt. Technol. Biomed. Life Sci.*, **784**, 101–109.
18. Hofer,A., Ekanem,J.T. and Thelander,L. (1998) Allosteric regulation of *Trypanosoma brucei* ribonucleotide reductase studied *in vitro* and *in vivo*. *J. Biol. Chem.*, **273**, 34098–34104.
19. Jia,S., Marjavaara,L., Buckland,R., Sharma,S. and Chabes,A. (2015) Determination of deoxyribonucleoside triphosphate concentrations in yeast cells by strong anion-exchange high-performance liquid chromatography coupled with ultraviolet detection. *Methods Mol. Biol.*, **1300**, 113–121.
20. Wanrooij,P.H., Tran,P., Thompson,L.J., Carvalho,G., Sharma,S., Kreisel,K., Navarrete,C., Feldberg,A.L., Watt,D.L., Nilsson,A.K. *et al.* (2020) Elimination of rNMPs from mitochondrial DNA has no effect on its stability. *Proc. Natl. Acad. Sci. U.S.A.*, **117**, 14306–14313.
21. Rentoft,M., Lindell,K., Tran,P., Chabes,A.L., Buckland,R.J., Watt,D.L., Marjavaara,L., Nilsson,A.K., Melin,B., Trygg,J. *et al.* (2016) Heterozygous colon cancer-associated mutations of SAMHD1 have functional significance. *Proc. Natl. Acad. Sci. U.S.A.*, **113**, 4723–4728.
22. Hirumi,H. and Hirumi,K. (1989) Continuous cultivation of *Trypanosoma brucei* blood stream forms in a medium containing a low concentration of serum protein without feeder cell layers. *J. Parasitol.*, **75**, 985–989.
23. Ciulli,A., Lobley,C.M., Tuck,K.L., Smith,A.G., Blundell,T.L. and Abell,C. (2007) pH-tuneable binding of 2′-phospho-ADP-ribose to ketopantoate reductase: a structural and calorimetric study. *Acta Crystallogr. D. Biol. Crystallogr.*, **63**, 171–178.
24. Pogolotti,A.L. and Santi,D.V. (1982) High-pressure liquid chromatography–ultraviolet analysis of intracellular nucleotides. *Anal. Biochem.*, **126**, 335–345.
25. Nakajima,K., Kitazume,S., Angata,T., Fujinawa,R., Ohtsubo,K., Miyoshi,E. and Taniguchi,N. (2010) Simultaneous determination of nucleotide sugars with ion-pair reversed-phase HPLC. *Glycobiology*, **20**, 865–871.
26. Behmüller,R., Forstenlehner,I.C., Tenhaken,R. and Huber,C.G. (2014) Quantitative HPLC-MS analysis of nucleotide sugars in plant cells following off-line SPE sample preparation. *Anal. Bioanal. Chem.*, **406**, 3229–3237.
27. Sieberth,V., Rigg,G.P., Roberts,I.S. and Jann,K. (1995) Expression and characterization of UDPGlc dehydrogenase (KfiD), which is encoded in the type-specific region 2 of the Escherichia coli K5 capsule genes. *J. Bacteriol.*, **177**, 4562–4565.
28. Oka,T. and Jigami,Y. (2006) Reconstruction of de novo pathway for synthesis of UDP-glucuronic acid and UDP-xylose from intrinsic UDP-glucose in Saccharomyces cerevisiae. *FEBS J.*, **273**, 2645–2657.
29. Schmidt,T.T., Sharma,S., Reyes,G.X., Kolodziejczak,A., Wagner,T., Luke,B., Hofer,A., Chabes,A. and Hombauer,H. (2020) Inactivation of folylpolyglutamate synthetase Met7 results in genome instability driven by an increased dUTP/dTTP ratio. *Nucleic Acids Res.*, **48**, 264–277.